Fast Tissue Segmentation Based on a 4D Feature Map: Preliminary Results

Simon Vinitski, Ph.D.[1*], Tad Iwanaga, M.S.[1], Carlos Gonzalez, M.D.[1], David Andrews, M.D.[2], Robert Knobler, M.D.[3], John Mack, M.S.

Thomas Jefferson University Hospital
Department of Radiology[1], Neurosurgery[2] and Neurology[3]
*132 S. 10th Street, Room 1098, Main Building, Philadelphia, PA 19107
215-955-7293 (FAX) 215-955-5329

Abstract. The primary aim of this work was to develop a fast and accurate method for tissue segmentation based on a 4D feature map to be used in stereotactic neurosurgery and the evaluation of multiple sclerosis, MS. Secondly, we wanted to validate our method with biological tissue studied in-vivo obtained by biopsy. Tissue segmentation based on both 3D and 4D feature maps were derived from high resolution MR images and was performed in five normal individuals, six patients with MS plaques in the brain, and six patients with malignant brain tumors from which four had undergone stereotactic biopsy. Three inputs: proton density, T2, and T1-weighted MR images were routinely utilized. As a fourth input, magnetization transfer was used in some patients, and T1-weighted post contrast MRI in others.

To speed up computation, our k-Nearest Neighbor segmentation algorithm was optimized by: 1) discarding redundant seed points, 2) discarding points within one half of a standard deviation from the cluster center that were non-overlapping with other tissue classes, and 3) discarding outlying seed points located beyond five standard deviations from the cluster center of each tissue class.

After segmentation, a stack of color-coded segmented images was created. Our new technique, utilizing all four MRI inputs provided better segmentation than that based on only three inputs. The tissues were smoother due to the reduction of statistical noise, and the delineation of the tissues was increased. Details that were previously blurred or invisible now became apparent. For example, in normal persons detailed depiction of deep gray matter nuclei was obtained. In malignant tumors, up to five abnormal tissues were identified: 1) solid tumor core, 2) cystic tumor, 3) white matter edema, 4) gray matter edema, and 5) tissue necrosis. Subsequent stereotactic biopsy and histological analysis confirmed the results of the tissue segmentations. In MS patients, delineation of MS plaque became much sharper.

In conclusion, the proposed 4D methodology warrants further development and clinical evaluation.

Key Words: MRI, tissue segmentation, 4D feature map, brain tumor, multiple sclerosis.

1 Introduction

The present work deals with the application of multispectral segmentation for the characterization of biological tissue using MR imaging. Segmentation, using three-dimensional (3D) display of magnetic resonance (MR) images of the head, is a prerequisite for recognition of the multiple tissue surfaces needed for surgical planning. Medical diagnosis with MR involves visual classification of tissues into separate groups using both medical experimentation and anatomic knowledge. However, a quantitative classification is required before automatic segmentation and the construction of a 3D surface map of anatomical features. The gray level thresholding that is commonly used to extract bone surfaces in CT images does not work well in the more complex MR images of the head because different tissues have overlapping intensity ranges.

Previously, we utilized the method of Cline et al (1). We used probability and connectivity on two sets of images (proton density and T2-weighted) to segment brain tissues. Although the two input model produces relatively good results (1,2), in order to better characterize the brain tissue, we introduced a multispectral analysis approach with three inputs, along with the k-Nearest Neighbor (k-NN) segmentation algorithm (3,4). The three sets of MRI data we used were: proton density, T2-weighted fast spin echo, and T1-weighted spin echo. We hypothesized and proved that the T1 contribution introduced substantial new pathophysiological information and provided, greater cluster separation in 3D feature space leading to better tissue segmentation (4). For example, we have used this technique in the identification of plaques of multiple sclerosis (MS), in different stages of demyelination. We also demonstrated the utility of this technique in following the course of MS and success of its treatment (5). Furthermore, we validated our 3D method with biological tissue obtained by biopsy, that had been studied in-vivo. We utilized an animal model of virus-induced brain tumor. Strong correlation between our model and histopathological results of tumor and brain tissue was also demonstrated (6). In this study our aims were: a) to develop a fast tissue segmentation protocol based on a 4D feature map, and b) have it compared with that based on a 3D feature map. Two alternatives were used as the fourth input for the 4D segmentation; T1-weighted post-gadolinium contrast images or images obtained by magnetization transfer (MT).

Gadolinium DTPA consists of small paramagnetic macromolecules which penetrate a defective brain/blood barrier in the brain and malignant brain tumor tissues. The area of penetration appears enhanced on a T1-weighted MRI (7). In contrast, Magnetization Transfer (MT) (8,9), is an effective method for changing the tissue contrast by selective saturation of the macromolecular bound water pool (short-T2 molecules) by RF pulses. This alters the magnetization properties of the long-T2 molecules (free water pool), which are in constant exchange with the bound water pool. Reduction in the apparent T1 and "mobile proton density" occur in biological tissues providing a new type of contrast mechanism. Numerous studies have demonstrated this effect in neuro-MRI (9).

We also wanted to compare our segmentation results with histologically confirmed specimens. In this regard, we investigated malignant tumors. We used the

topographical distribution for each pathological tissue in question, extracted from our color-coded segmented images, to perform stereotactic biopsies in patients with malignant tumors. Histological evaluation of these biopsy specimens were performed and the results were compared to those obtained through segmentation analysis.

2 Methods and Materials

Imaging was performed on 1.5 T sigma scanner. To immobilize patients a special collar was used. Phantom experiments were also performed. Five samples, which represented the CSF, white/gray tissues, blood and fat, were utilized as a phantom image. MRI was performed in five normal volunteers, six patients with cerebral MS, and six patients with malignant brain tumors. In the normal volunteers the fourth input was magnetization transfer (MT). In the patients with tumors or MS, the fourth input used was either MT or T1 post Gadolinium. Four patients with Gadolinium post-contrast images underwent stereotactic biopsy. The imaging parameters were as follows: proton density and T_2-weighted images were obtained from fast spin echo (TR=5sec, TE_1/TE_2=15/105 msec, ETL=8, BW=62kHz), T1 weighted spin-echo was the third input (TR/TE=500/11msec) and MT magnetization transfer was obtained using a manufacturer supplied pulse sequence. Offset resonance was 1500 Hz.

After imaging, data was transferred to Sun Sparc Station 10 for processing. The application of our methodology to stereotactic intracranial biopsies was performed in the following fashion. The patient was placed in the stereotactic frame and immediately underwent MR imaging. Next, a qualified observer seeded training points. The computation time took 1-2 minutes. Previously, this step took 3-9 hours for even a 3D feature map. The neurosurgeon and neuroradiologist visually examined the stack of color-coded images. The biopsy points (for the different pathological tissues) were selected and their coordinates were recorded by a dedicated stereotactic computer. This computer was in the operating room to provide precision stereotactic coordinates for the intracranial biopsy.

As we stated earlier, a supervised k-NN method was employed (10). For each tissue class, 20-50 points were taken by an expert neuroradiologist. Using the seed points, 3D and 4D feature maps were calculated.

The k-NN algorithm computes the Euclidean distance of pixel intensities between an unclassified pixel and seed points (sample points). The unclassified point is determined to belong to the tissue class of the nearest neighbor. To further speed up classification time, if a classified pixel intensity was within the non-overlapping distance from the centroid of each center (that was used for thinning sample points), the Euclidean distance of intensities between an unclassified point and the centroid of each tissue class was used.

To further speed up computation, our k-NN algorithm was optimized by: 1) discarding redundant seed points, 2) discarding points within one half of a standard deviation from the cluster center that were non-overlapping with other tissue classes,

and 3) discarding outlying seed points locating beyond five standard deviations from the cluster center of each tissue class.

After segmentation, a stack of color-coded segmented images was created, and up to ten tissues were classified. A connectivity algorithm (11), along with a dividing cube algorithm (12), constructs a surface of selected tissue(s). Optionally, a median filter and an anisotropic filter (square) can be applied before classification (13). A misaligned image was corrected, when needed, by shifting and rotating the image horizontally and vertically until it was aligned with the other images. In brief, differences between old and new images was minimized.

3 Results

In our previous tissue segmentation method based on a 3D feature map (4, 5), computation time (using a Sparc station 10), was between 5-8 hours, depending on the number of seeding points. In the current model, based on a 4D feature map, computation time (using a Sparc station 20), was reduced to 1-2 minutes. Such an increase in speed, in the present technique, has been extremely important for the applicability of this technique in patient management. For example, patients with brain tumors can be operated upon shortly after the MRI has been performed.

Segmentation analysis based on 3D and 4D feature maps produced excellent discrimination of normal and abnormal tissues. In the normal brain, for example, separation of different components of the basal ganglia was obtained in spite of close similarity of the histology of these tissues. MT image (TR/TE= 1700/20) was, usually, used as a fourth input. It should be emphasized that the segmented image based on the 4D feature map, showed significantly better details of the deep gray matter nuclei, whose structure was clearly identified. Caudate Nuclei, Globus Pallidus, Thalamus, Internal Capsule (white matter), CSF, and Cortical gray matter. To the best of our knowledge no such detailed segmentation of the basal ganglia has been published in the literature (14). It can be noted that distribution of some tissues are very close to each other, particularly at the edge of the image. Therefore, further refinement is needed to correct this problem. However, images based on a 4D feature map are noticeably cleaner than those based on a 3D feature map. Excellent separation of other normal brain tissues such as the gray matter, white matter and cerebrospinal fluid (CSF), was also obtained in all of the normal volunteers.

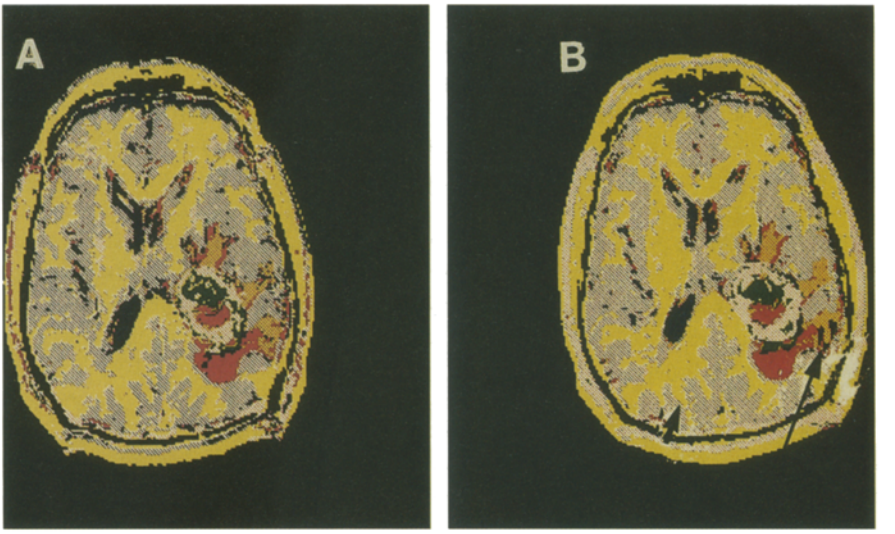

Fig. 1. Segmented images of a left posterior temporal glioblastoma multiforme. **A:** Based on 3D feature map. **B:** Based on 4D feature map. Four abnormal tissues are seen within the area of the tumor: irregular ring vascular enhancing tissue (pink); necrotic areas (red); areas of increased cellularity (green); perivascular edema (green). Normal tissue include normal white matter (yellow), normal gray matter (gray) and CST (blue). Notice that the image obtained with segmentation based on 4D feature map is significantly sharper, clearer, and have more information. The gray matter (short arrow), as well as boundary between tumoral tissue, and CSF (long arrow) are more completely visualized.

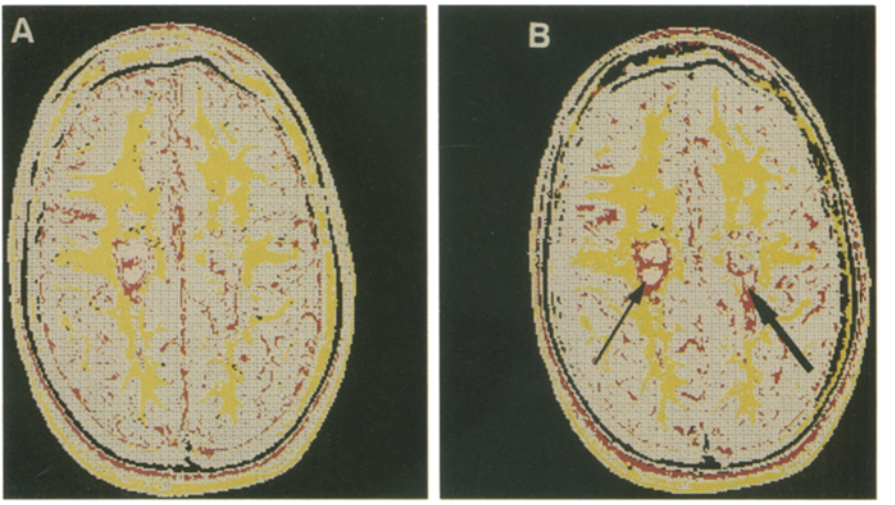

Fig. 2. Segmented images of the brain of a patient with progressive multiple sclerosis. **A:** Based on 3D feature map; **B:** Based on 4D feature map. Two well defined abnormal tissues are visualized within the plaque, the central gliotic area (pink) and peripheral demyelination (red). Normal tissues include normal white matter (yellow) and normal gray matter (gray). Notice that the image based on 4D feature map is sharper, clearer and have more information (thin arrow). Areas of demyelination not visualized with 3D are clearly well visualized in 4D (thick arrow).

In the analysis of brain tumors, discrimination abnormal tissues was even more striking (Figure 1). Edema surrounding the tumor was visualized in all cases, but more importantly, the interface between tumor tissue and edema was clearly demarcated. These findings were even more clearly appreciated in the segmentation based on a 4D feature map. This border zone area is very difficult to identify in conventional MRI scans and is very important for the surgeon in planning the extent of surgery and radiosurgery. Areas of necrosis, cystic formation and solid tissue within the tumor were accurately identified in all cases and confirmed by stereotactic biopsy and histology. Excellent correlation was obtained between the tissues within the tumor observed by MRI segmentation and the tissues obtained from biopsy of these areas. Consequently, this technique can safely be used by the neurosurgeon in determining the tumor areas he wants to sterotactically biopsy before surgery. In the analysis of the MS patients, similar advantages of 4D over 3D were seen, mainly in the identification and characterization of the MS plaques (Figure 2).

Segmentation analysis based on a 4D feature map also produced significantly better definition and outline of anatomical and pathological structures as result of a better characterization of the tissues. As compared to segmentation based on a 3D feature map, where irregularities and fuzziness of the borders are present, segmentation based on the 4D feature map is significantly sharper. Even more importantly was the significant reduction of statistical noise (random color points) obtained with the technique based on a 4D feature map. These findings can also be readily appreciated in most segmented images.

We used T1-contrast-enhanced post -MR images in one group of patients as the fourth segmentation parameter, and magnetization transfer in another group of patients. The results of the segmentation were different since two different techniques were used to increase the contrast between the tissues. In the first case, the properties of the tissue were modified by injection of a paramagnetic contrast media. In the second case , enhanced contrast was obtained by magnetization transfer, a method based on selective saturation of the macromolecular bound water pool with time (7,9). The enhancing tissues were readily identified in the segmentation when gadolinium was injected, whereas only relative mild changes were detected in the segmentation when magnetization transfer was used. However, in this study our aim was not to optimize MT parameters, or any other fourth parameter but to obtain segmented images based on a 4D feature map, as fast as possible, to compare it with that based on a 3D feature map.

4 Discussion

In clinical practice, the accurate identification of different tissues within close proximity is an invaluable asset in establishing the correct diagnosis and facilitating the application of appropriate therapy. Quantitation of these measures allows assessment of the response to treatment over time. The introduction of a fourth input was based on the assumption that cluster separation would be increased in 4D feature space. Therefore, additional imaging time to address possible misregistration was

worthwhile. Indeed, in previous experiments, when the number of dimensions was increased from two to three, the accuracy of volumetric measurements phantoms, as well as tissue segmentation, increased. These results were statistically significant (4).

With the addition of T1 information (as the third input), segmented images demonstrated two subtypes of tissues within MS plaques. We presume that these two different types of tissues most likely represent the different stages involved in the evolution of the MS lesion, such as: gliosis vs. MS demyelination with edema. Investigation of MS plaque substructure using a 4D feature map technique will be continued.

It should be emphasized that the present images are preliminary, and were performed only to test the ability of our method to rapidly produce segmented images based on either a 3D or 4D feature map. Some segmented images are somewhat noisy, particularly at the edges. This problem requires further refinement of our technique. A number of approaches will be taken. Probably, the most important will be the correction of RF inhomogeneity as proposed by Mohamed et al (15). This technique is particularly effective at the edges of the coil, and has been successfully tested in our previous results (2-6). In the present study, images were processed using an eight bit gray scale. As our next step, we will investigate the effect of applying a16 bit gray scale. We estimate that the consequent increase in computation time will not exceed 30%.

Another major factor not completely addressed in this work, was the optimization of pulse sequences and imaging parameters. Nonetheless, as we previously predicted, images based on a 4D feature map showed better results with, smoother tissue boundaries in the segmentations due to the decrease in statistical noise (random color points) and, sharper tissue delineation.

Finally, the most important finding of the present study was the strong correlation between results of our tissue segmentation technique, based on the four MR image inputs, and histological examination of stereotactically obtained biopsy specimens. Our results suggest that segmented images, displayed in 3D space, can assist neurosurgeons prior to and, more importantly, during the actual surgery or stereotactic biopsy. Moreover, our technique can be used as a quantitative indicator of disease evolution or drug response in MS and other lesions.

In conclusion, this study indicates that our method of tissue segmentation based on a 4D tissue map substantially improved segmentation results as compared with that based on a 3D feature map. Moreover, these results were in full accord with histopathological examination. Another important result is the improved speed of computation, allowing use of this technique, for the "real time" applications. Consequently, further technical and clinical evaluation is warranted.

References

1. Cline HE, Lorensen WE, Kikinis R, Jolesz F. 3D segmentation of MR images of the head using probability and connectivity. J CAT 14:1037-1042, 1990.

2. Vinitski S, Gonzalez C, Burnett C, Seshagiri S, Mohamed FB, Lublin FD, Knobler RL, Frazer G. Tissue segmentation by high resolution MRI: improved accuracy and stability. Proc. IEEE Eng. Med. Biol. 16:577-578, 1994.
3. Vinitski S, Seshagiri S, Mohamed FB, et al. Tissue characterization by MR: data segmentation using 3D feature map. In: Vernazza G, Venetsanopoulos AN, Bracccini C (eds), Image processing theory and applications. Amsterdam: Elsevier Science Publishers B.V., 325-328, 1993.
4. Vinitski S, Gonzalez C, Mohamed FB, et al. "Improved intracranial lesion characterization by tissue segmentation based on a 3D feature map." Magn Reson Med 37:457-469, 1996.
5. Vinitski S, Gonzalez C, et al. "Tissue Segmentation in MRI as an Informative Indicator of Disease Activity in the Brain" In: DeFloriani L., Vernazza G, (eds), Image Analysis Processing. Berlin: Springer-Verlag, 265-270, 1995.
6. Vinitski S, Gonzalez C, et al. Validation of 3D Tissue Segmentation by Animal Model of Brain Tumor. Proc. IEEE Eng. Med. Biol. 18:606.1-606.3, 1996.
7. R. Brasch, MRI Contrast Enhancement in the Central Nervous System: A Case Study Approach, Raven Press, N.Y. 1993.
8. S Vinitski, R.H Griffey et al., Lactate Observation by Spectral Editing, "Magn. Reson. Imag. 6:707-710, 1988.
9. B.S. Hu, S.M Connely et al., "Pulsed saturation transfer contrast,"Magn. Reson. Med 26:231-228, 1992.
10. T.M. Cover and P.E. Hart, classification "IEEE Transaction on Information Theory", Vol. 13, 1967. pp 21-27, Nearest Neighborhood Pattern.
11. Cline HE, Dumoulin CL, et al. 3D reconstruction of the brain from MRI using a connectivity algorithm. Magn Reson Imaging 5:345-349, 1987.
12. Cline HE, Lorensen WE, Ludke S, Crawford CR. Two algorithms for the three-dimensional reconstruction of tomograms. Med Phys 15:320-327, 1988.
13. G. Gerig, et al., Nonlinear Anisotropic Filtering of MRI Data, IEEE Transaction on Medical Imaging Vol. II. No.2, 1992.
14. Proceedings of the NIH Workshop "Evaluation of multiple sclerosis lesion load: Comparison of segmentation image processing techniques," held at Montreal Neurological Institute, November 6-7, 1995.
15. Mohamed FB, Vinitski S, Gonzalez C, Faro S, Burnett C, Ortega HV, Iwanaga T. "Image nonuniformity correction in high field (1.5T) MRI." Proc IEEE Eng Med Bio 17:36-37, 1995.
16. Gonzalez C, Mitchell DR, Sacchetti T, Seward JD, Knobler RL, Lubin FD: Correlation between structural brain lesions and emotional and cognitive function in patients with multiple sclerosis: an MRI study. Neuroradiology; (suppl) 123-124, 1991.
17. Vinsitski S, Iwanaga T, Gonzalez C, Andrews D, Knobler R, Mack J, Madi S. "Tissue Segmentation Based on a 4D Feature Map". Proceed of the Fifth Meeting of the International Society for Magnetic Resonance in Medicine, Vancouver, BC, April 15-20, 1997; 476.